



Motor domain-based motility system and motile properties of alpha heavy chain in *Tetrahymena* outer arm dynein



Masaki Edamatsu *

Department of Life Sciences, Graduate School of Arts and Sciences, The University of Tokyo, Tokyo, Japan

ARTICLE INFO

Article history:

Received 23 September 2014

Available online 5 October 2014

Keywords:

Tetrahymena

Ciliated protozoan

Ciliary motility

Cytoskeletal protein

Biomolecular motor

Axonemal dynein

ABSTRACT

Axonemal dynein plays an essential role in ciliary motility, and impaired ciliary motility causes human diseases such as primary ciliary dyskinesia (PCD). The motor domain of axonemal dynein powers ciliary motility and its function is regulated by several accessory proteins bound to the tail region. Therefore, to understand the essential properties of dynein motility, examining the motile properties of the motor domain without the tail is necessary. In this study, the functional motor domain of the alpha heavy chain in *Tetrahymena* outer arm dynein was purified, and its motile properties were examined using an *in vitro* motility system. The purified protein caused microtubules to glide at a velocity of 5.0 $\mu\text{m/s}$ with their minus-end trailing, and motility was inhibited in an ATP concentration-dependent manner, which is in contrast with kinesin1. This method could be applicable to other axonemal dyneins and will enable further molecular studies on diverse axonemal dyneins and ciliary motility.

© 2014 Elsevier Inc. All rights reserved.

1. Introduction

In motile cilia and flagella, nine peripheral doublet microtubules surround the central pair of singlet microtubules (9 + 2 structure). The peripheral doublets are associated with outer and inner arm dyneins that produce the force required for ciliary and flagellar motilities. Dysfunction of axonemal dynein causes the most prominent ciliopathy, primary ciliary dyskinesia (PCD), which is associated with respiratory symptoms, male infertility and *situs inversus* [1–3].

Dynein is a large AAA+ ATPase and is divided into a catalytic motor domain and a tail region [4,5]. The motor domain contains four P-loops implicated in ATP hydrolysis, and the tail binds to peripheral doublet microtubules and several accessory proteins such as intermediate chains (IC) and light chains (LC) that regulate dynein function.

Axonemal dyneins have unique properties that are not found in other motor proteins. In ciliary beating, the dyneins on doublet microtubules must be locally activated in a coordinated manner to generate a ciliary waveform. In addition, the motility of axonemal dyneins is affected by the concentration of ATP and/or ADP [6,7]. In *Tetrahymena*, permeabilized cells were shown to swim in a wide range of ATP concentrations but were immotile

in concentrations higher than 7 mM ATP, and somatic axonemes trembled in an uncoordinated fashion at high ATP concentrations [6]. ATP concentration-dependent inhibition has also been observed in other organisms [6,7]. Axonemal dyneins have been implicated in this phenomenon, but the molecular mechanism underlying this process remains to be elucidated.

Recently, a functional expression and *in vitro* motility system of axonemal dynein heavy chain (HC) has been developed in *Tetrahymena* [8,9]. Although this expression system is useful for functional and structural studies of axonemal dyneins, another motility system is still needed to investigate the essential properties of dynein motility because the purified protein contains a second microtubule-binding site in the tail and is associated with several accessory proteins, such as ICs and LCs, that regulate dynein function.

In this study, the functional motor domain of axonemal dynein was purified, and an *in vitro* motility system for the motor domain was established and revealed the unique motile properties of the alpha HC of *Tetrahymena* outer arm dynein.

2. Materials and methods

2.1. Strains and culture conditions

Wild-type *Tetrahymena thermophila* strains B2086.1 and CU428.1 were obtained from the Stock Center for *T. thermophila* at Cornell University (Ithaca, NY, USA). *Tetrahymena* cells were

* Address: Department of Life Sciences, Graduate School of Arts and Sciences, The University of Tokyo, 3-8-1 Komaba, Meguro-ku, Tokyo 153-0041, Japan.

E-mail address: cedam@mail.ecc.u-tokyo.ac.jp

grown in SPP medium (1% protease peptone, 0.1% yeast extract, 0.2% glucose and 0.003% Fe-EDTA) at 30 °C.

2.2. Construction of the expression cassette and transformation

The genomic sequence of the DYH3 gene (gene ID: TTHERM_01276420) was obtained from the *Tetrahymena* Genome Database (TGD) Wiki (<http://ciliate.org/index.php/home/welcome>). The expression cassette was constructed as previously described [9]. The F1 (1.8-kb untranslated region of DYH3), neo (neomycin resistance gene), BTU1P (beta-tubulin 1 promoter) and F2 (6.8-kb tail region of DYH3, HRV-FLAG-TtBCCP and 2.2-kb fragment of DYH3 motor domain) regions were sequenced and sequentially introduced into the pGBKT7 vector (Clontech; Santa Clara, CA, USA). The PCR primers used in this study are listed in Supplemental Table S1. Transformation was performed as previously described [8].

2.3. PCR analysis

Genomic DNA was isolated as previously described [8]. The primers for PCR analysis are listed in Supplemental Table S1. The PCR products were analyzed using agarose gel electrophoresis and visualized by GR Green nucleic acid stain (LabSupply; Dunedin, New Zealand). Homologous recombination was also confirmed by sequencing the corresponding region.

2.4. Fluorescence microscopy

Permeabilized *Tetrahymena* cells were prepared as previously described [6]. The permeabilized cells were incubated with 30 nM Cy3-streptavidin (Life Technologies; Tokyo, Japan) for 30 min on ice and observed by fluorescence microscopy (BX60, Olympus; Tokyo, Japan).

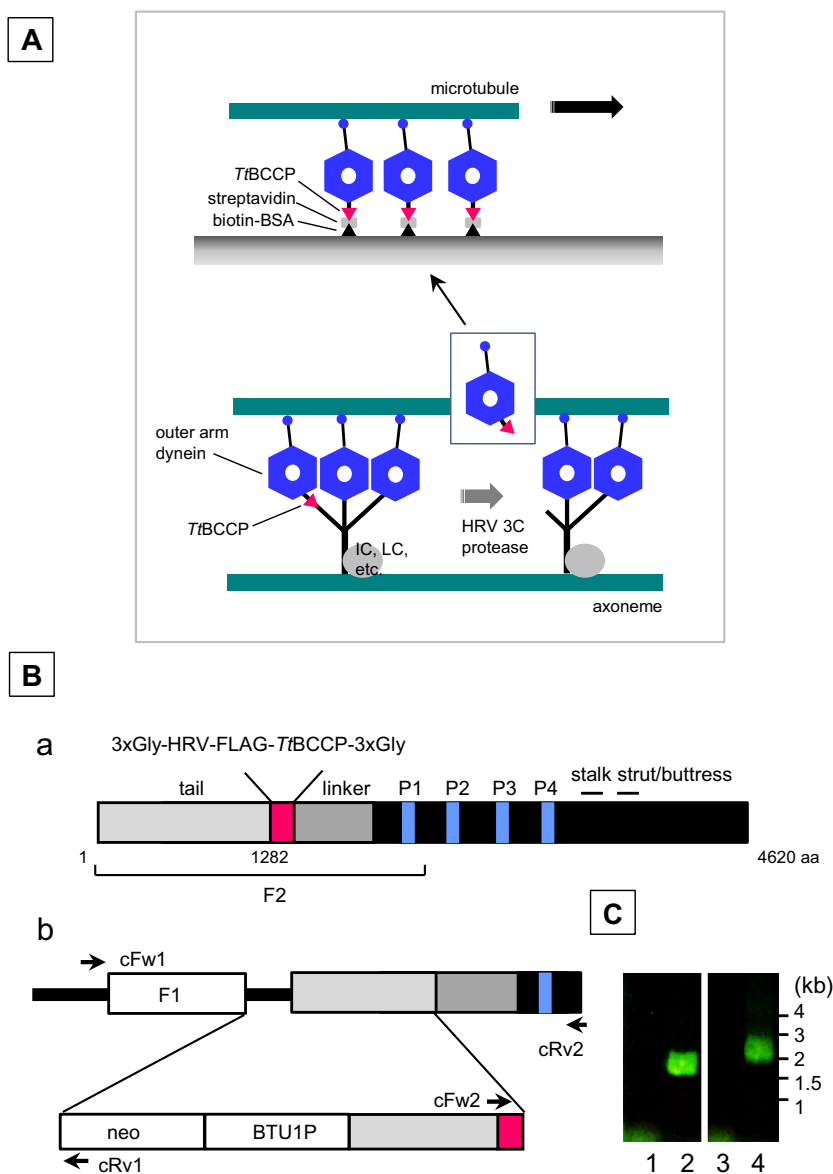


Fig. 1. Motor domain-based motility system. (A) Schematic representation of the purification and motility system. (B) Construction of the expression cassette and PCR analysis. (a) Domain structure of DYH3. The bracket shows the region used for the expression cassette. (b) Homologous recombination of the expression cassette into the DYH3 locus. The arrows represent the positions of the primers used in the PCR analysis. (C) PCR analysis. Lanes 1 and 2: PCR using cFw1 and cRv1 primers; lanes 3 and 4: PCR using cFw2 and cRv2 primers. Lanes 1 and 3: wild-type; lanes 2 and 4: transformant.

2.5. Purification of DYH3 motor domain

The transformant was grown to the stationary phase in SPP medium containing 40 µg/ml paromomycin at 30 °C, with agitation. The axoneme was prepared as previously described [10], and digested using HRV 3C protease (Takara; Shiga, Japan) in preparation buffer (10 mM HEPES pH 7.4, 100 mM NaCl, 4 mM MgCl₂, 1 mM EGTA and 0.1 mM PMSF) for 4 h at 4 °C. The supernatant was incubated with anti-FLAG M2 affinity gel (Sigma–Aldrich; Tokyo, Japan) for 2 h at 4 °C on a rotator. The gel was washed several times using preparation buffer containing 0.1% Nonidet-P40, and the motor domain of DYH3 was then eluted with 0.5 mg/ml 3× FLAG peptide (Sigma–Aldrich) for 30 min on ice.

2.6. Avidin-blot analysis

The axonemes were prepared as previously described [10]. Axonemal proteins and purified proteins were separated using SDS–PAGE, transferred to a nitrocellulose membrane and detected using Cy3–streptavidin or horseradish peroxidase–streptavidin (Sigma–Aldrich).

2.7. Preparation of tubulin and polarity-marked microtubules

Tubulin was purified from porcine brain as previously described [11]. Polarity-marked microtubules labeled with X-rhodamine succinimidyl ester (Life Technologies) were prepared as previously described [12].

2.8. In vitro motility assays

The gliding assay was performed in assay buffer (10 mM PIPES pH 7.0, 5 mM MgSO₄, 1 mM EGTA, 1 mM DTT, 0.02–5 mM ATP and 10 µM paclitaxel) under a dark-field microscope or fluorescence microscope as previously described [8]. The flow chamber was sequentially coated with biotinylated BSA (Sigma–Aldrich), streptavidin (Wako; Osaka, Japan) and casein (Sigma–Aldrich) to specifically immobilize the motor domain of DYH3. The gliding velocity and motile direction were examined as previously described [8]. For one control experiment, rat kinesin1 (amino acids 1–430) fused to AviTag (Avidity; Colorado, USA) at the C-terminus was used instead of the DYH3 described above. For a second control, native outer arm dynein was non-specifically absorbed onto a glass slide, and the flow chamber was blocked with casein.

3. Results

The motor domain of alpha HC of *Tetrahymena* outer arm dynein (DYH3) must be purified from axonemes because the functional motor domain cannot be prepared from cytoplasmic extract. The experiment is outlined in Fig. 1A. The HRV 3C protease site, FLAG-tag and *Tt*BCCP surrounded by 3× Gly were inserted tandemly at the N-terminal of the DYH3 motor domain (Fig. 1A and B). The three-headed outer arm dyneins were digested in the axoneme by HRV 3C protease and recovered using anti-FLAG resin. The purified protein was fixed onto a glass slide by *Tt*BCCP and examined in the *in vitro* motility system (Fig. 1A).

The DYH3 construct used in this study is shown in Fig. 1B. The bracket corresponds to the fragment used for the expression cassette. The PCR primers used in this study are shown in Supplemental Table S1. Homologous recombination was confirmed by PCR analysis (Fig. 1B and C).

It was essential for the recombinant dynein to be biotinylated and localized in the axoneme, and the localization of the dynein was examined by fluorescent microscopy using Cy3–streptavidin

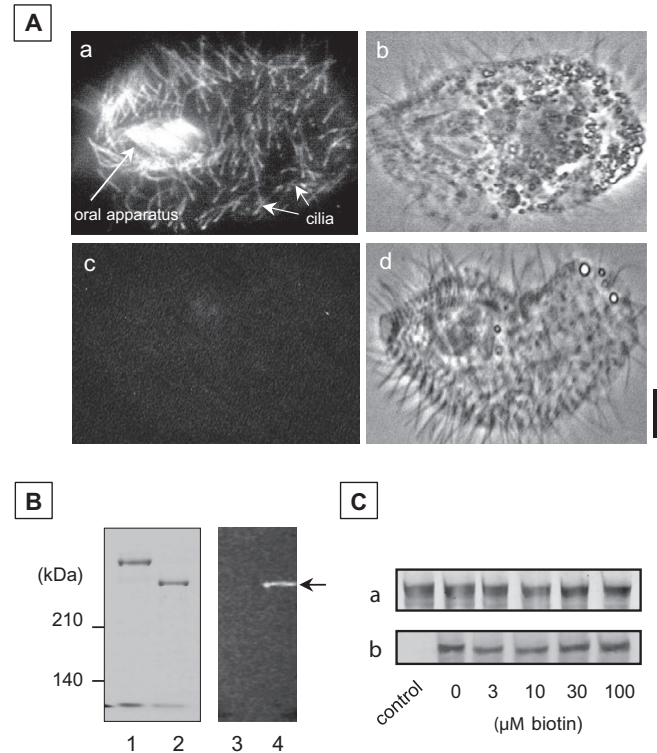


Fig. 2. Localization and purification of the DYH3 motor domain. (A) Localization of the DYH3 motor domain in *Tetrahymena* cells. (a and b) Cy3-SA staining; (c and d) preincubation with 5 mM biotin; (a and c) fluorescence images; (b and d) phase-contrast images. The scale bar represents 10 µm. (B) Purification and avidin-blot analysis of the motor domain of DYH3. Lanes 1 and 2: CBB staining; lanes 3 and 4: Cy3-SA staining. Lanes 1 and 3: native outer arm dynein; lanes 2 and 4: motor domain of DYH3. (C) Biotinylation of DYH3. Axonemal proteins were prepared and analyzed by SDS–PAGE (a) and avidin-blot analysis (b).

(Cy3-SA). Permeabilized cells were incubated with Cy3-SA to brightly label the cilia and oral apparatus (Fig. 2A). In the control experiments, fluorescence in the cilia and oral apparatus was quenched by preincubation of Cy3-SA with 5 mM biotin (Fig. 2A). This result indicated that the recombinant dynein was biotinylated and localized in the axoneme.

To purify the DYH3 motor domain, the axoneme was incubated with HRV 3C protease, and the motor domain was recovered using anti-FLAG resin. The purified protein had a higher mobility than the native outer arm dynein on SDS–PAGE and was specifically labeled with Cy3-SA, confirming it to be the biotinylated motor domain of DYH3 (Fig. 2B). Biotinylation of the dynein was performed in standard protease peptone medium, and the addition of 0–100 µM biotin to the medium did not significantly enhance the biotinylation of the dynein (Fig. 2C).

Next, the motility of the DYH3 motor domain was assayed *in vitro* (Fig. 1A). Biotinylated BSA, streptavidin, casein, DYH3 motor domain, and microtubules were introduced sequentially into the flow chamber. The motor domain was fixed on glass slides via streptavidin–biotin binding. The gliding velocity was 5.0 ± 1.0 µm/s (average velocity \pm SEM), which was similar to that of native outer arm dynein (Fig. 3A). In control experiments, few microtubules were found in the flow chamber after preincubation with 5 mM biotin (Fig. 3A). This work was the first to purify the functional motor domain of axonemal dyneins. Recently, it was found that the motile direction of a certain microtubule-based motor switched following the partial deletion of the region corresponding to the DYH3 tail [13], and thus the motile direction of the DYH3 motor domain was determined. The purified protein moved polarity-marked microtubules with their minus-end

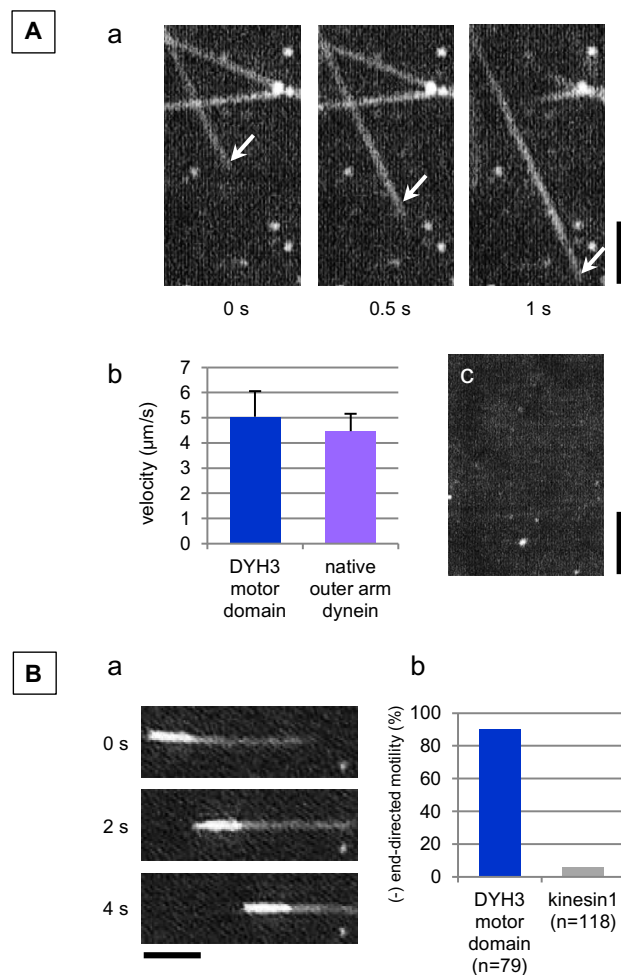


Fig. 3. Gliding assay of the DYH3 motor domain. (A) (a) Gliding of microtubules. The arrows indicate a gliding microtubule. The scale bar represents 3 μm. (b) Bar graph of gliding velocities. The error bar represents the SEM. (c) Control experiment: the flow chamber was preincubated with 5 mM biotin prior to the introduction of the DYH3 motor domain. The scale bar represents 10 μm. (B) (a) Movement of a polarity-marked fluorescent microtubule. The scale bar represents 3 μm. (b) Bar graph of motile directions. The percentages of the total microtubules moving in the minus-end direction are shown.

lagging, indicative of minus-end-directed motility, which is the same direction as outer arm dynein (Fig. 3B).

Ciliary and flagellar motility were inhibited by high concentrations of ATP, as described above, but the dynein species implicated in the ATP concentration-dependent inhibition has not yet been identified. Therefore, the motility of DYH3 was examined in various ATP concentrations. As a result, the rate of gliding microtubules among total microtubules (gliding index) decreased at high ATP concentrations. In 0.02–1 mM ATP, the gliding index was higher than 0.90, but it decreased to 0.65 in 2 mM ATP and to 0.020 in 5 mM ATP, in contrast with kinesin1 (Fig. 4A). The dark-field images showed that many microtubules were found in the flow chamber in 0.02 mM ATP, whereas most microtubules were detached from the glass slide in 5 mM ATP (Fig. 4B). The remaining microtubules in the flow chamber did not glide but mostly fluctuated in 5 mM ATP (Fig. 4B).

4. Discussion

This study established a motor domain-based motility system and demonstrated the unique properties of the alpha HC of

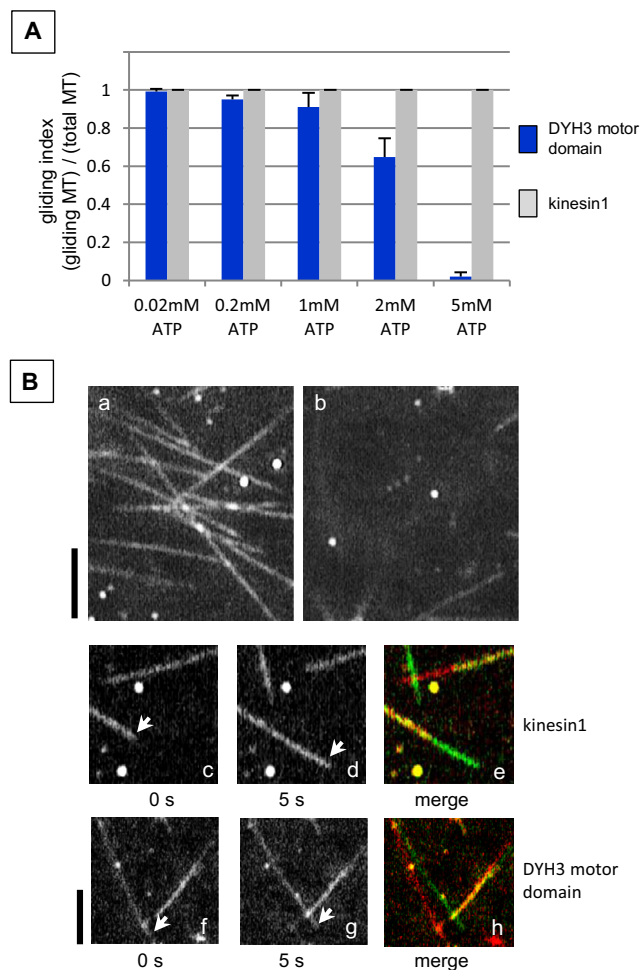


Fig. 4. ATP concentration-dependent inhibition. (A) Bar graph of gliding index. Gliding indices of the DYH3 motor domain (blue) and kinesin1 (gray) are shown. The error bar represents the SEM. (B) Gliding assay. Dark field images in 0.02 mM ATP (a) and 5 mM ATP (b). The scale bar represents 5 μm. (c–e) Gliding assay of kinesin1 in 5 mM ATP. The arrows represent gliding microtubules. (f–h) Gliding assay of the DYH3 motor domain in 5 mM ATP. The arrows represent fluctuating microtubules. The scale bar represents 3 μm.

Tetrahymena outer arm dynein. The tail of axonemal dynein binds to microtubules and several accessory proteins that regulate the function of axonemal dynein. This motility system eliminates the effect of the tail and allows for the investigation of the essential motile properties of axonemal dynein. It is necessary for the functional purification of motor domain to use axonemes as a starting material because the motile motor domain could not be prepared from cytoplasmic extract. The *in situ* digestion method using HRV 3C protease had an advantage in avoiding contamination with other ciliary proteins.

The TtBCCP tag was recently identified in *Tetrahymena* and applied to an *in vitro* motility assay of outer arm dynein [9]. TtBCCP is also applicable to the motor domain-based motility system, and this small tag at the N-terminal of the DYH3 motor domain efficiently fixed the motor domain on a glass slide via avidin–biotin binding. The HRV protease site, FLAG-tag and TtBCCP could be introduced into another region of axonemal dynein and used for various molecular studies of the dynein.

High concentrations of ATP are known to inhibit ciliary and flagellar motility [6,7]. In *Tetrahymena*, permeabilized cells did not swim, and their cilia trembled in ATP concentrations higher than 7 mM. In addition, permeabilized *Chlamydomonas* cells exhibited

immotile or circling behavior in more than 10 mM ATP [6]. Four nucleotide-binding loops (P-loops) in certain axonemal dyneins are thought to play key roles in the ATP concentration-dependent inhibition, but the dynein species involved in the phenomena has not yet been identified.

This study showed that DYH3 exhibited ATP concentration-dependent inhibition. The gliding index decreased in high ATP concentrations, and most microtubules did not glide in 5 mM ATP. In *Tetrahymena*, permeabilized cells swam in 5 mM ATP at a speed similar to that in 1 mM ATP [6], which appeared to be inconsistent with the ATP concentration-dependence of DYH3. These results suggested that there is another dynein species with different ATP concentration-dependent inhibition from DYH3. In addition, the tail of DYH3 was found to not be essential for the ATP concentration-dependent inhibition. *Tetrahymena* has 23 axonemal dynein heavy chain genes [14], and which dynein species has the ATP concentration-dependent inhibition and how the ciliary motility is inhibited by those dyneins at high ATP concentrations are of interest.

Most microtubules were detached from the glass slide in 5 mM ATP in this gliding assay. During the ATP hydrolysis cycle, dynein is thought to strongly bind to microtubules in the apo- (or ADP-) state and weakly bind to microtubules in the ADP.Pi- (or ATP-) state. A recent report indicated that nearly half of the outer arm dyneins in the axoneme were in the apo-state even under conditions that induce the ADP.Pi-state [15], and similar findings have been revealed in an *in vitro* reconstituted system using pig brain microtubules [16]. Thus, it is possible that a large portion of the DYH3 motor domain was in the apo-state under low ATP concentrations and therefore strongly bound to microtubules in the gliding assay. The dyneins would bind to the microtubules much more weakly in the gliding assay if induced completely from the apo-state into the ADP.Pi-state. To elucidate the detaching mechanism of the microtubules, it is important to examine the state of the dyneins on microtubules at high ATP concentrations in the gliding assay.

This motor domain-based method is useful for examining the essential motile properties of axonemal dyneins without the influence of the tails and could be applicable to diverse axonemal dyneins. Currently, *Tetrahymena* is the only expression system for functional axonemal dyneins, and this motility system will enable

further molecular studies of diverse axonemal dyneins and ciliary motility.

Appendix A. Supplementary data

Supplementary data associated with this article can be found, in the online version, at <http://dx.doi.org/10.1016/j.bbrc.2014.09.127>.

References

- [1] P. Satir, S.T. Christensen, Structure and function of mammalian cilia, *Histochem. Cell Biol.* 129 (2008) 687–693.
- [2] J.L. Badano, N. Mitsuma, P.L. Beales, N. Katsanis, The ciliopathies: an emerging class of human genetic disorders, *Annu. Rev. Genomics Hum. Genet.* 7 (2006) 125–148.
- [3] W.F. Marshall, The cell biological basis of ciliary disease, *J. Cell Biol.* 180 (2008) 17–21.
- [4] R.D. Vale, AAA proteins. Lords of the ring, *J. Cell Biol.* 150 (2000) F13–F19.
- [5] R. Kamiya, Functional diversity of axonemal dyneins as studied in *Chlamydomonas* mutants, *Int. Rev. Cytol.* 219 (2002) 115–155.
- [6] U.W. Goodenough, Motile detergent-extracted cells of *Tetrahymena* and *Chlamydomonas*, *J. Cell Biol.* 96 (1983) 1610–1621.
- [7] A. Yoshimura, I. Nakano, C. Shingyoji, Inhibition by ATP and activation by ADP in the regulation of flagellar movement in sea urchin sperm, *Cell Motil. Cytoskeleton* 64 (2007) 777–793.
- [8] M. Edamatsu, The functional expression and motile properties of recombinant outer arm dynein from *Tetrahymena*, *Biochem. Biophys. Res. Commun.* 447 (2014) 596–601.
- [9] M. Edamatsu, Identification of biotin carboxyl carrier protein in *Tetrahymena* and its application in *in vitro* motility systems of outer arm dynein, *J. Microbiol. Methods* 105 (2014) 150–154.
- [10] T.M. Gibson, D.J. Asai, Isolation and characterization of 22S outer arm dynein from *Tetrahymena* cilia, *Methods Cell Biol.* 62 (2000) 433–440.
- [11] M.D. Weingarten, A.H. Lockwood, S.Y. Hwo, M.W. Kirschner, A protein factor essential for microtubule assembly, *Proc. Natl. Acad. Sci. USA* 72 (1975) 1858–1862.
- [12] A. Hyman, D. Drechsel, D. Kellogg, S. Salser, K. Sawin, P. Steffen, L. Wordeman, T. Mitchison, Preparation of modified tubulins, *Methods Enzymol.* 196 (1991) 478–485.
- [13] M. Edamatsu, Bidirectional motility of the fission yeast kinesin-5, Cut7, *Biochem. Biophys. Res. Commun.* 446 (2014) 231–234.
- [14] D.E. Wilkes, H.E. Watson, D.R. Mitchell, D.J. Asai, Twenty-five dyneins in *Tetrahymena*: a re-examination of the multidynein hypothesis, *Cell Motil. Cytoskeleton* 65 (2008) 342–351.
- [15] T. Movassagh, K.H. Bui, H. Sakakibara, K. Oiwa, T. Ishikawa, Nucleotide-induced global conformational changes of flagellar dynein arms revealed by *in situ* analysis, *Nat. Struct. Mol. Biol.* 17 (2010) 761–767.
- [16] A. Maheshwari, T. Ishikawa, Heterogeneity of dynein structure implies coordinated suppression of dynein motor activity in the axoneme, *J. Struct. Biol.* 179 (2012) 235–241.